# QCD Chiral Phase Diagram from Weak fRG Equation

< INT Workshops in Autumn 2025>

**Yuepeng Guan**

（玥鹏  关）

*Center for Theoretical Physics and College of Physics, Jilin University*

November 3rd, 2025

Based on: **Y. G.** and Masatoshi Yamada, 2510.25081 [hep-ph].

# Content

- **Introduction**
- **Functional renormalization group (fRG) setup**
  - FRG setups for QCD fermionic potential: LPA’
  - Gluonic sector and running coupling
- **Searching for the weak solution of fRG equations**
  - Why divergence of 4-fermi matters?
  - Weak form of the RG equations
  - Rankine-Hugoniot condition
  - Method of characteristics
- **Results and discussions**
- **Summary**
- **References**

# Content

- Introduction
- **Functional renormalization group (fRG) setup**
  - FRG setups for QCD fermionic potential: LPA’
  - Gluonic sector and running coupling
- **Searching for the weak solution of fRG equations**
  - Why divergence of 4-fermi matters?
  - Weak form of the RG equations
  - Rankine-Hugoniot condition
  - Method of characteristics
- **Results and discussions**
- **Summary**
- **References**

# Introduction

- Quantum Chromodynamics (QCD) and its (chiral) phase structure

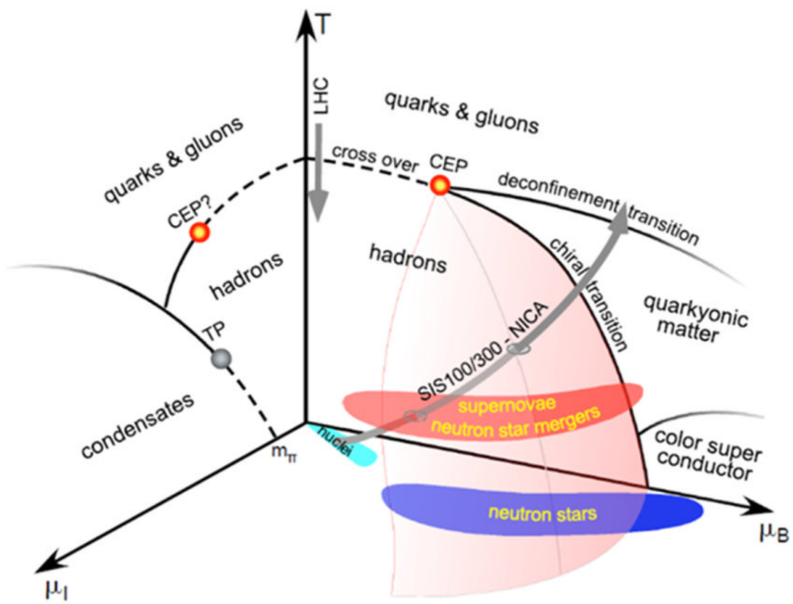


[1] Peter Senger. Probing dense QCD matter in the laboratory—The CBM experiment at FAIR. Phys. Scripta, 95(7):074003, 2020

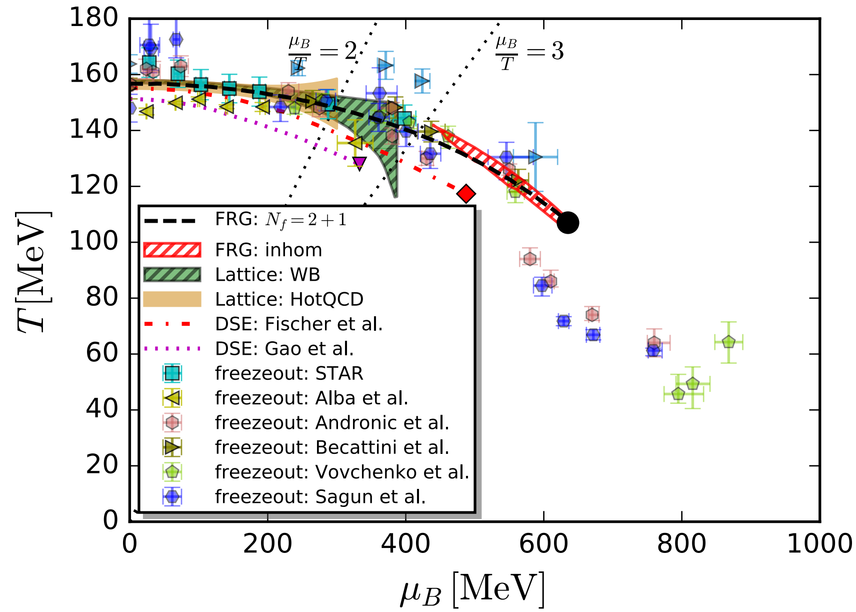


[2] Wei-jie Fu, Jan M. Pawlowski, and Fabian Rennecke. QCD phase structure at finite temperature and density. Phys. Rev. D, 101(5):054032, 2020.

# Introduction

- Renormalization group acrossing the critical scale [3]

E.g.: RG flow of 4-fermion coupling in massless gauged-NJL, with fixed gauge coupling.

$$\partial_t \tilde{G}_S = -2\tilde{G}_S + A\tilde{G}_S^2 + B\tilde{G}_S\alpha_s + C\alpha_s^2$$

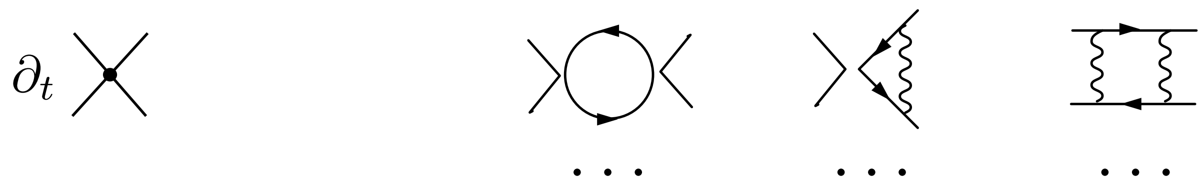


Flowing structure and phases:

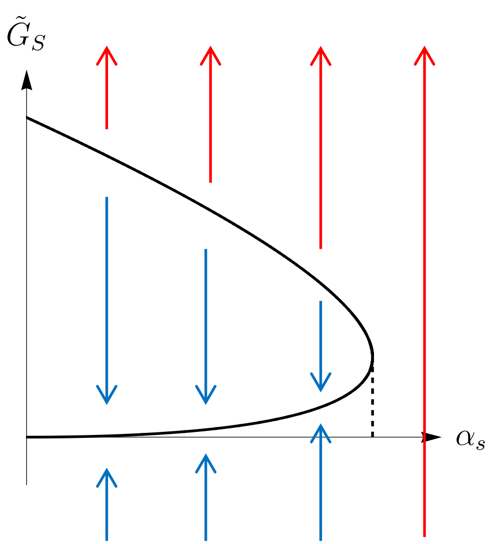


$$\Longrightarrow$$

Flow w.r.t. RG scale:

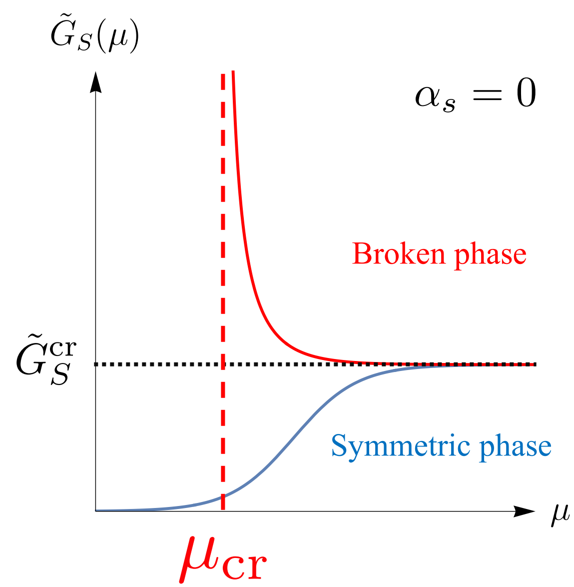


Divergence of the 4-fermion coupling

$\Downarrow$

Signal of Spontaneous Chiral Symmetry breaking

# Introduction

○ Dynamical bosonization and meson fluctuations

4-fermion coupling?

Chiral susceptibility!

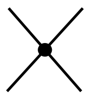

$$\sim \frac{\delta^2 \Gamma_k}{\delta\left(\bar\psi\psi\right)\delta\left(\bar\psi\psi\right)} \qquad \chi = \frac{1}{\mathcal{V}}\frac{\partial^2 W_k}{\partial m^2} = \int_x \left\langle \left(\bar\psi\psi\right)_x \left(\bar\psi\psi\right)_0 \right\rangle_k$$

Divergence arised from the massless mode propagation:

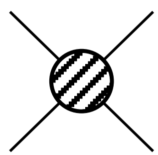

$$\ni$$

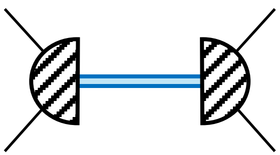

$$\sim \frac{1}{p^2}$$

Emergence of the mesonic resonances: See, e.g, W.-j. Fu, et al. [2] and J. Braun, et al. [4].

$$\partial_t \phi_k^a(p) = \int_q \boxed{\partial_t \mathcal{A}_k(q-p,q)}\,\bar\psi(q-p)\Gamma^a\psi(q)$$

$$\Downarrow$$

Enters the flow, tunned to absorb the flow of 4-fermion

# Introduction

- Question:

Is the mesonic fluctuations necessary to get into the broken phase?

- "Conclusion" from this work:

No in principle, and yes in practice.

- No: See, e.g, K.-I. Aoki, et al. [5].

  Weak solution of fRG.

- Yes: See, e.g W.-J. Fu, et al. [2].

  Mesonic fluctuation and chiral criticality

- In this work:
  - Functional renormalization group (fRG) equation for QCD (fermion) in the medium;
  - Local potential approximation (LPA) and its modification, ladder and non-ladder approximations.
  - Weak solution;
  - Phase diagram in $(\mu_B, T)$-plane.

# Content

- **Introduction**
- **Functional renormalization group (fRG) setup**
  - FRG setups for QCD fermionic potential: LPA’
  - Gluonic sector and running coupling
- **Searching for the weak solution of fRG equations**
  - Why divergence of 4-fermi matters?
  - Weak form of the RG equations
  - Rankine-Hugoniot condition
  - Method of characteristics
- **Results and discussions**
- **Summary**
- **References**

# FRG setup

○ FRG setups for QCD fermionic potential: LPA'

Mean-field approximation

QCD action at UV:

$$S_{\text{bare}}[\Phi] = \int_x \left[ \frac{1}{4} F^a_{\mu\nu} F^a_{\mu\nu} + \frac{1}{2\xi} (\partial_\mu A^a_\mu)^2 + \bar{\psi}(\not{\partial} + i g_s \not{A} - m_l - \mu_q \gamma_4) \psi \right]$$

QCD action at IR:

$$\Gamma_k[\Phi] = \int_x \left[ \frac{Z^A_k}{4} F^a_{\mu\nu} F^a_{\mu\nu} + \frac{Z^A_k}{2\xi} (\partial_\mu A^a_\mu)^2 + Z^\psi_k \bar{\psi}(\not{\partial} + i g_s \not{A} - \mu_q \gamma_4) \psi - V_k(\psi, \bar{\psi}) \right]$$

- Flow equation of average one-partical effective action (1PIEA)

Wetterich equation [6]:

$$\partial_t \Gamma_k[\Phi] = \frac{1}{2} \mathrm{STr} \left[ \left( \Gamma^{(2)}_k + \mathcal{R}_k \right)^{-1} \partial_t \mathcal{R}_k \right]$$

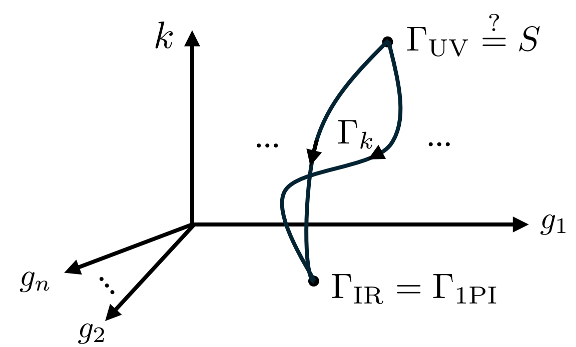

# FRG setup

- Regulator function: sharp cutoff $t = \log(k/\Lambda)$

$$\mathcal{R}_k^\psi(|\boldsymbol{p}|) = Z_k^\psi i\not{\boldsymbol{p}} r_k^\psi(|\boldsymbol{p}|/k),$$
$$\mathcal{R}_k^A(|\boldsymbol{p}|) = Z_k^A \boldsymbol{p}^2 r_k^\psi(|\boldsymbol{p}|/k),$$
$$r_k^A = r_k^\psi = \frac{1}{\theta(|\boldsymbol{p}|/k - 1)} - 1$$

$$\partial_t \Gamma_k[\Phi] = -\frac{1}{2}\int_{p,\mathrm{shell}} \mathrm{str}\log\Gamma_k^{(2)}$$

$$\Gamma_{k,a,b}^{(2)} = \begin{pmatrix} H_{BB} & H_{BF} \\ H_{FB} & H_{FF} \end{pmatrix}$$

$$\int_{p,\mathrm{shell}} \equiv T\sum_{n=-\infty}^{\infty}\int \frac{\mathrm{d}^3\boldsymbol{p}}{(2\pi)^3} \underbrace{k\delta(|\boldsymbol{p}|-k)}_{\partial_t \mathcal{R}_k}$$

- Fierz subspace projection $\sigma = \bar{\psi}\psi$

$$V_k(\psi,\bar{\psi}) \ni (\bar{\psi}\lambda^I\psi)^2 + (\bar{\psi}\lambda^I i\gamma_5\psi)^2 + \cdots \quad \Longrightarrow \quad V_k(\psi,\bar{\psi}) \equiv V(\sigma;t)$$

- Large-N leading order

$$\frac{\overrightarrow{\delta}}{\delta\psi^T(-p_\psi)}\mathcal{V}_k^\psi\frac{\overleftarrow{\delta}}{\delta\psi(q_\psi)} \to 0, \quad \frac{\overrightarrow{\delta}}{\delta\bar{\psi}(p_\psi)}\mathcal{V}_k^\psi\frac{\overleftarrow{\delta}}{\delta\bar{\psi}^T(-q_\psi)} \to 0,$$

$$\frac{\overrightarrow{\delta}}{\delta\psi^T(-p_\psi)}\mathcal{V}_k^\psi\frac{\overleftarrow{\delta}}{\delta\bar{\psi}^T(-q_\psi)} \to +\mathbf{1}_{\mathrm{total}}\int_x e^{-i(p_\psi-q_\psi)}\partial_\sigma V(\sigma), \quad \frac{\overrightarrow{\delta}}{\delta\bar{\psi}(p_\psi)}\mathcal{V}_k^\psi\frac{\overleftarrow{\delta}}{\delta\psi(q_\psi)} \to -\mathbf{1}_{\mathrm{total}}\int_x e^{-i(p_\psi-q_\psi)}\partial_\sigma V(\sigma).$$

# FRG setup

- General structure of the flow equation

$$\partial_t V(\sigma;t) - \eta_\psi \sigma \partial_\sigma V(\sigma;t) = -\frac{1}{2}\int_{p,\mathrm{shell}} \mathrm{tr}\left[\log S^{-1}(p_\psi^-) + \log\left(S^{(T)}(p_\psi^+)\right)^{-1}\right] + \frac{1}{2}\int_{p,\mathrm{shell}} \mathrm{tr}'\log\left\{\delta^{ab}\delta_{\mu\nu} + \mathcal{A}^{ab}_{\mu\nu} + \mathcal{B}^{ab}_{\mu\nu}\right\}$$

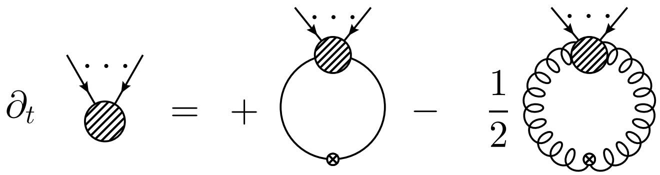


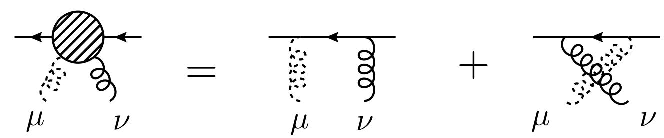


- Truncating the loops: “ladder” and “non-ladder” approximations

$$\mathrm{tr}'\log(1+\mathcal{A}+\mathcal{B}) = -\sum_{n=1}^{\infty}\frac{(-1)^n}{n}\,\mathrm{tr}'\left(\mathcal{A}+\mathcal{B}\right)^n$$

E.g.: (Part of) RG flow of 4-fermion coupling.

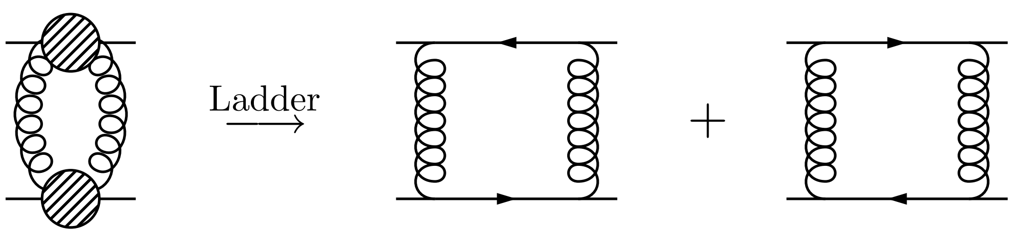


Non-ladder diagram:

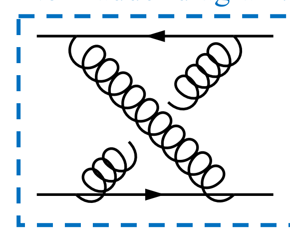

Color factors: $\left(\frac{C_2}{4N_c}\right)^2 N_c \propto N_c$ $\qquad$ $\left(\frac{C_2}{4N_c^2}\right) \propto \frac{1}{N_c}$

# FRG setup

- Partial defferential equations [7] $\partial_t V(\sigma;t) = -F(\partial_\sigma V, \sigma; t)$

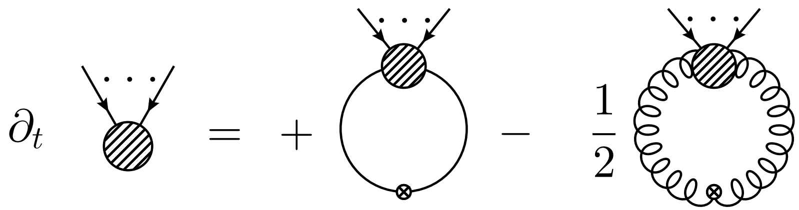

$$\partial_t V(\sigma;t) - \eta_\psi \sigma \partial_\sigma V(\sigma;t) = -\frac{1}{2}\int_{p,\mathrm{shell}} \mathrm{tr}\left[\log S^{-1}(p_\psi^-) + \log\left(S^{(T)}(p_\psi^+)\right)^{-1}\right] + \frac{1}{2}\int_{p,\mathrm{shell}} \mathrm{tr}' \log\left\{\delta^{ab}\delta_{\mu\nu} + \mathcal{A}^{ab}_{\mu\nu} + \mathcal{B}^{ab}_{\mu\nu}\right\}$$

Ladder:

$$\begin{aligned}\partial_t V(\sigma;t) &= \eta_\psi \sigma \partial_\sigma V(\sigma;t)\\ &- T\sum_n \frac{k^3}{2\pi^2}\log\left(\omega_{\psi,n}^2 + (\sqrt{k^2+\mathcal{M}^2} - \mu_q)^2\right)\\ &- T\sum_n \frac{k^3}{2\pi^2}\log\left(\omega_{\psi,n}^2 + (\sqrt{k^2+\mathcal{M}^2} + \mu_q)^2\right),\end{aligned}$$

Non-ladder:

$$\begin{aligned}\partial_t V(\sigma;t) &= \eta_\psi \sigma \partial_\sigma V(\sigma;t)\\ &- \frac{1}{2}\left[\mathrm{Flow}_k^{\mathrm{N.L.},-}(\sigma, M_\psi) + \mathrm{Flow}_k^{\mathrm{N.L.},+}(\sigma, M_\psi)\right].\end{aligned}$$

Now, the fermionic sector is ready, leaving gluonic sector (gauge coupling) unknown.

# FRG setup

## ○ Gluonic sector and running coupling

- Difficulty: running coupling

Missing: 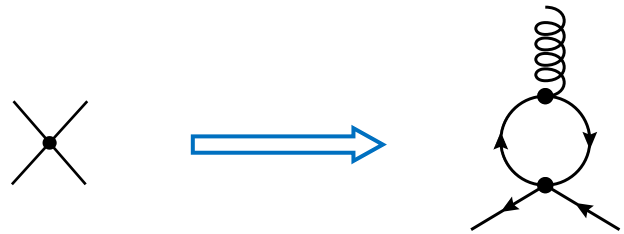 is not accessable…

- (Quark-gluon) gauge coupling as input

Renormalized gauge coupling:

$$\alpha_s = \frac{1}{Z_k^A}\frac{\bar{g}_s^2}{4\pi}$$

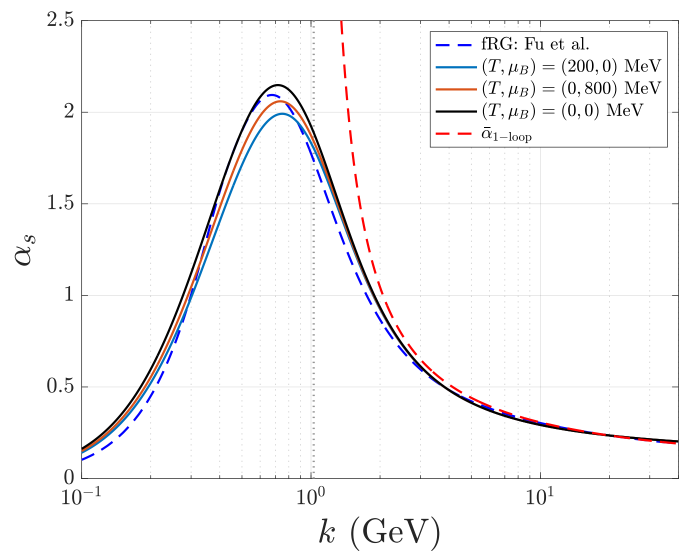

# FRG setup

- Quantitative result of the quark-gluon dressing

$$\bar{g}_s(k) = \lambda^{(1)}_{\bar{q}Aq}(\bar{p} = k)$$

Padé approximation to fit the runng coupling [8]:

$$\bar{g}_s(k) = \frac{0.2301 + 0.4411\,k + 0.3967\,k^2}{0.0832 + 0.0838\,k + 0.4502\,k^2}$$

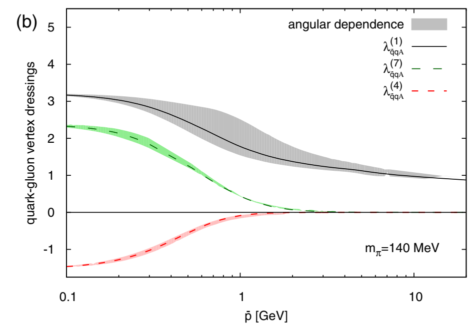


A. K. Cyrol, et al. [8]

- Quantitative result of the gluon propagator wave function

$$Z_k^A = Z^{\text{trans}}_{T,\mu_q}(p = k)$$

HTL approximation to the thermal mass
(quark vacuum polarization):

$$Z^{\text{trans}}_{T,\mu_q}(p) = Z_{\text{vac}}(p) + \frac{4\pi}{3}\alpha_S^{\text{HTL}}\left(T^2 + \frac{3}{\pi^2}\mu_q^2\right)\frac{1}{p^2}$$

Gluon dressing at vanishing temperature and quark chemical potential: (see, e.g., F. Gao, et al. [9].)

$$Z^{-1}_{\text{vac}}(k^2) = \frac{k^2\,\frac{a^2+k^2}{b^2+k^2}}{M_G^2(k^2) + k^2\left[1 + c\log(d^2k^2 + e^2M_G^2(k^2))\right]^{\gamma}}$$

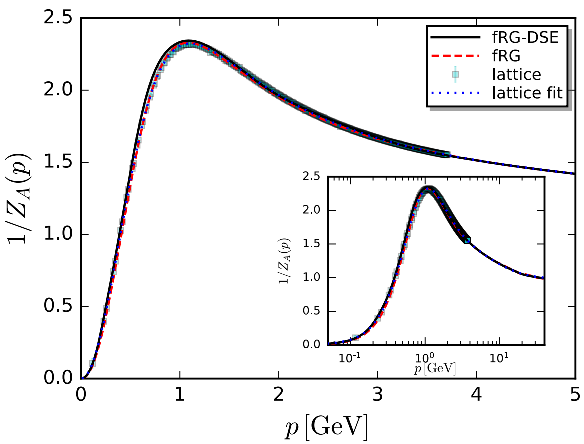


F. Gao, et al. [9]

Flavor: (2+1) at physical point.

# FRG setup

- Rescale the gauge coupling: controlling IR quantities

$$\alpha_s \to \bar{\alpha}_s = s \cdot \alpha_s$$

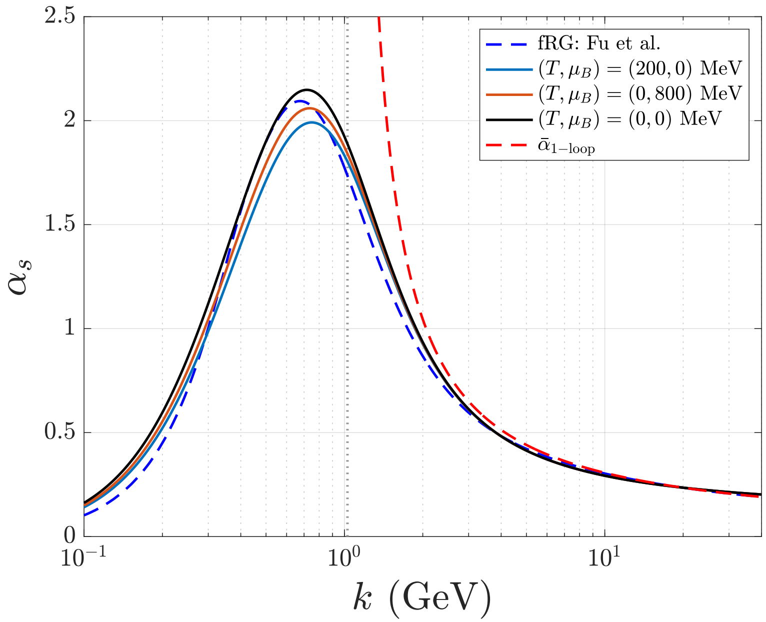


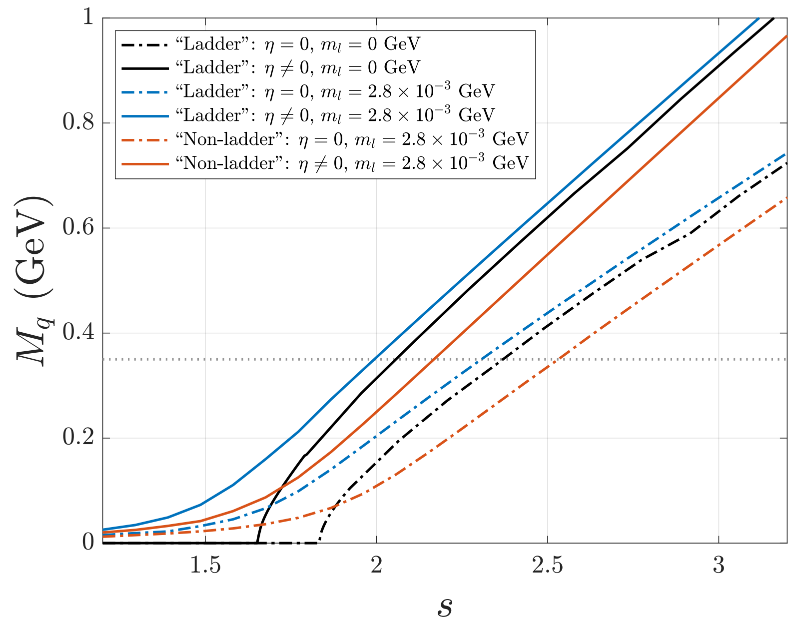


PDE closed.

# Content

- **Introduction**
- **Functional renormalization group (fRG) setup**
  - FRG setups for QCD fermionic potential: LPA'
  - Gluonic sector and running coupling
- **Searching for the weak solution of fRG equations**
  - Why divergence of 4-fermi matters?
  - Weak form of the RG equations
  - Rankine-Hugoniot condition
  - Method of characteristics
- **Results and discussions**
- **Summary**
- **References**

# Searching for the weak solution of fRG equations

## ○ Why divergence of 4-fermi matters?

$$\sigma = \bar{\psi}\psi$$

- Center object:

Fermionic potential

$$\partial_t V(\sigma; t) = -F(\partial_\sigma V, \sigma; t)$$

- Definning:

Mass function — 4-fermion coupling

$$M(\sigma; t) \equiv \partial_\sigma V(\sigma; t), \quad G(\sigma; t) \equiv \partial_\sigma^2 V(\sigma; t)$$

- "Problem" we meet:

E.g., chiral limit

$$\underbrace{\left| G(0^\pm; t_c^+) \right|}_{\text{Critical scale}} \to \infty \implies \begin{cases} \underbrace{M(0^+; t < t_c) \neq M(0^-; t < t_c)}_{\text{Discontinuity}} \\ \underbrace{\partial_\sigma V(0^+; t < t_c) \neq \partial_\sigma V(0^-; t < t_c)}_{\text{Non-analyticity}} \end{cases}$$

At some points, flow equation is not defined below the critical scale.

(* Possible solution: divide the field space, e.g.: K.-I. Aoki et al. PTEP, 2013:043B04 [7];

Singularities appears elsewhere @ finite chemical potential or beyond chiral limit. *)

# Searching for the weak solution of fRG equations

## ○ Weak form of the RG equations

- Original RG equation vs. weak form of the RG equation

$$\partial_t V(\sigma;t) = -F(\partial_\sigma V, \sigma; t)$$

Deformation: $\Downarrow \partial_\sigma$

Original RG: $$\partial_t M(\sigma;t) = -\partial_\sigma F(M(\sigma;t),\sigma;t) = -\frac{\partial F}{\partial M}\cdot\underline{\underline{\frac{\partial M}{\partial \sigma}}} - \frac{\partial F}{\partial \sigma}$$

"Conservation law"

Singularities at some points

Arbitary smooth test function

$$\lim_{\sigma\to\pm\infty}\varphi(\sigma;t) = 0, \quad \lim_{t\to-\infty}\varphi(\sigma;t) = 0$$

$$\Downarrow$$

Weak RG: $$\int_{-\infty}^{0} \mathrm{d}t \int_{-\infty}^{\infty} \mathrm{d}\sigma \, \underline{\underline{\left( M\frac{\partial\varphi}{\partial t} + F\frac{\partial\varphi}{\partial\sigma}\right) = -\int_{-\infty}^{\infty} \mathrm{d}\sigma \, (M\,\varphi)_{t=0}}}$$

Discontinuity is allowed!

- Weak solution of the weak RG equation

Mass function satisfies the weak RG equation is the *weak solution.*

- Containing finite numbers of discontinuity *points* ($\sigma$-direction);
- Satisfies the *original RG* elsewhere.

# Searching for the weak solution of fRG equations

## ○ Rankine-Hugoniot condition

- Condition for weak solution

$$\boxed{\left(M^{(L)} - M^{(R)}\right) \mathrm{d}\sigma^* = \left[F(M^{(L)}) - F(M^{(R)})\right] \mathrm{d}t.}$$

- Continuity condition from "conserved charge"

$$\begin{aligned}\mathrm{d}V^{(L/R)}(\sigma^*(t)) &= \left.\frac{\partial V}{\partial \sigma}\right|_{(L/R)} \mathrm{d}\sigma^* + \left.\frac{\partial V}{\partial t}\right|_{(L/R)} \mathrm{d}t \\ &= M^{(L/R)}\mathrm{d}\sigma^* - F(M^{(L/R)})\mathrm{d}t.\end{aligned}$$

$$\Downarrow$$

$$\mathrm{d}V^{(L)}(\sigma^*(t);t) - \mathrm{d}V^{(R)}(\sigma^*(t);t) = 0.$$

Potential stays continues during the flow.

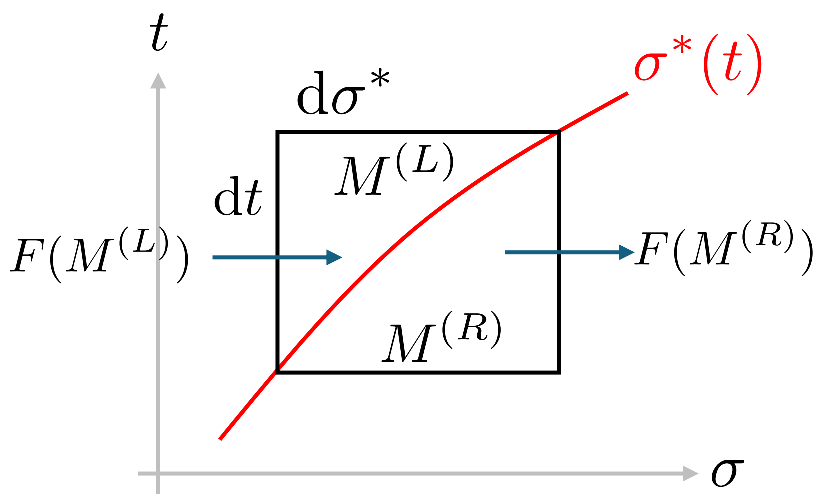


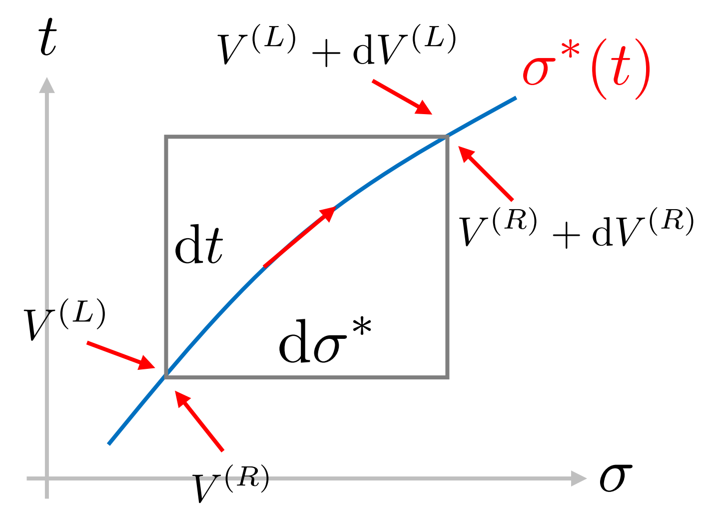

# Searching for the weak solution of fRG equations

- Extract weak solution according to RH condition

E.g.: solution of fermionic potential and mass function from NJL-type model @ finite chemical potential [10].

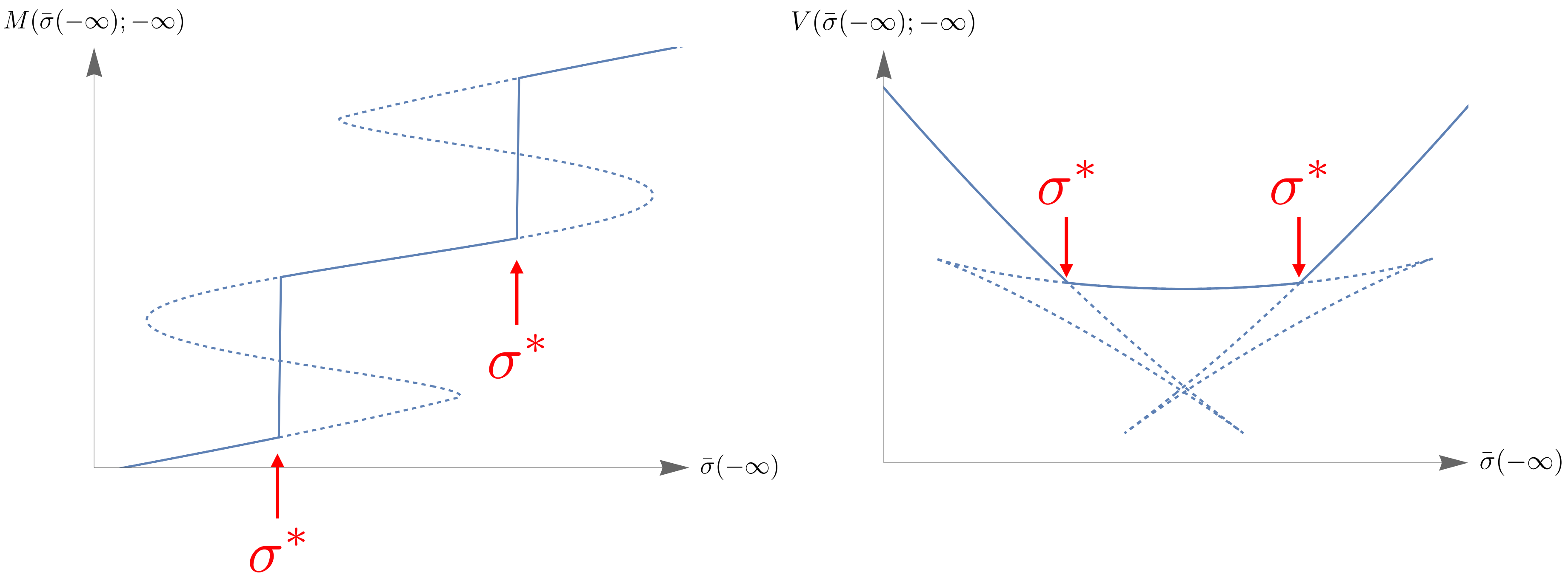


Determines the unique weak solution from a multi-values solution.

# Searching for the weak solution of fRG equations

## ○ Method of characteristics

Method of obtainning the **“strong” solution**.

- Characteristic curve in $(\sigma, t)$-plane

$$\frac{\mathrm{d}}{\mathrm{d}t}\bar{\sigma}(t) = \frac{\partial F(\bar{M}, \bar{\sigma}; t)}{\partial \bar{M}}$$

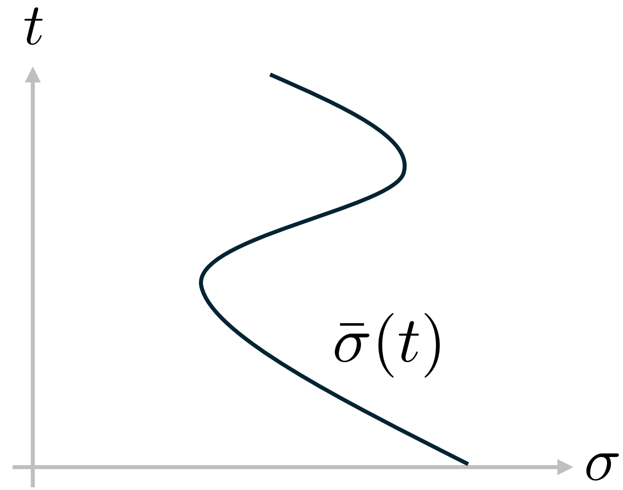


- PDE vs. coupled ODE

$$\begin{aligned}\frac{\mathrm{d}}{\mathrm{d}t}\bar{M} &= \left.\frac{\partial M(\sigma; t)}{\partial \sigma}\right|_{\sigma=\bar{\sigma}} \frac{\mathrm{d}}{\mathrm{d}t}\bar{\sigma} + \frac{\partial M(\bar{\sigma}; t)}{\partial t} \\ &= -\left.\frac{\partial F(M, \sigma; t)}{\partial \sigma}\right|_{\sigma=\bar{\sigma}}.\end{aligned}$$

$$\begin{cases} \bar{M} = \bar{M}(t) \\ \bar{\sigma} = \bar{\sigma}(t) \end{cases}$$

$$\begin{cases} \bar{\sigma}(0) = \sigma_0 \\ \bar{M}(0) = M_\Lambda(\sigma_0) \end{cases}$$

(Also the integral form of fermionic potential.)

# Searching for the weak solution of fRG equations

- Examples: laddar w/o. A.D., chiral limit @ T = 10 MeV

$k \in [40, 10^{-3})$ GeV

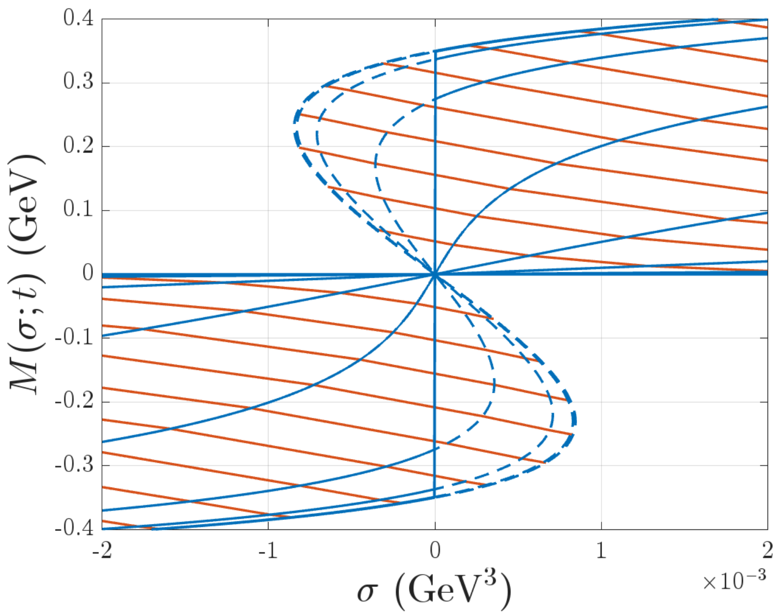


$\mu_B = 0$

$\mu_B \in \{1.1, 1.125, 1.139, 1.15, 1.175, 1.2\}$ GeV

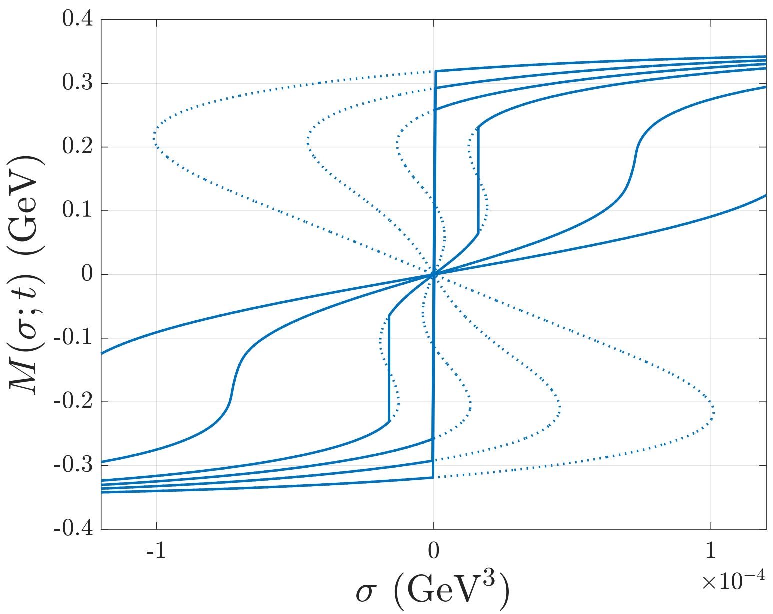


$k \sim 10^{-3}$ GeV

# Searching for the weak solution of fRG equations

- Strategy in this work


Get the **“strong” solution** for original RG.

Keeping the “**superium**” of the potential.

Extract **“physical quantities”** from weak RG.

- Numerical implement

Two coupled ODE, 5-th Runge-Kutta method with initial condition

$$\bar{\sigma}(0) = \sigma_0, \quad \bar{M}(\bar{\sigma}(0); 0) = m_l$$

We are ready.

# Content

- **Introduction**
- **Functional renormalization group (fRG) setup**
  - FRG setups for QCD fermionic potential: LPA'
  - Gluonic sector and running coupling
- **Searching for the weak solution of fRG equations**
  - Why divergence of 4-fermi matters?
  - Weak form of the RG equations
  - Rankine-Hugoniot condition
  - Method of characteristics
- **Results and discussions**
- **Summary**
- **References**

# Results and discussions

## ○ Quark mass function and parameter fixing

- Quark mass function with $p = k$

$$M_q(p) = \bar{M}(0; k = p)$$

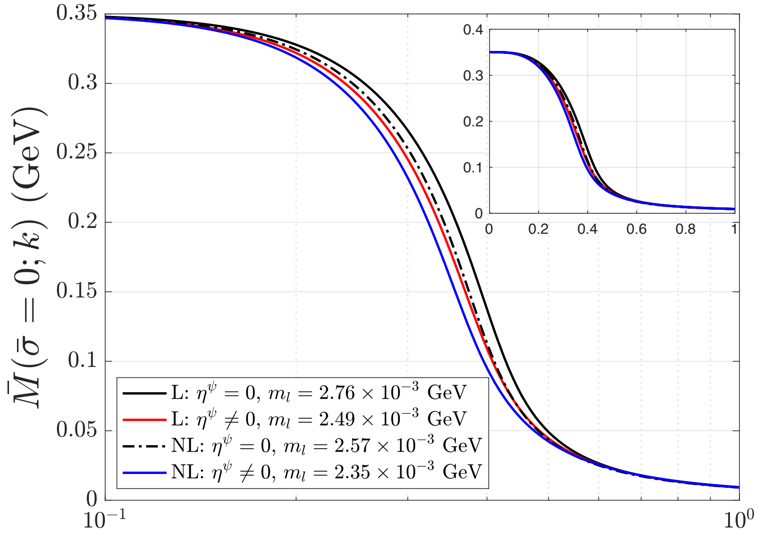


- Parameter fixing $(\bar{\alpha}_s, m_l)$

$$m_\sigma \sim 2\bar{M}(0; \infty) \equiv 2M_q$$

$$m_\pi^2 f_\pi^2 \sim 2m_l \langle \bar{\psi}\psi \rangle$$

where

$$f_\pi^2 = \frac{3}{\pi^2} \int_\kappa^\Lambda \mathrm{d}p \frac{p^3 M_q(p)}{\left[p^2 + M_q^2(p)\right]^2} \left[M_q(p) - \frac{p}{4}\partial_p M_q(p)\right]$$

$$\langle \bar{\psi}\psi \rangle = -\frac{N_c}{2\pi^2} \int_\kappa^\Lambda p^3 \mathrm{d}p \left[\frac{M_q(p)}{p^2 + M_q^2(p)} - \frac{m_l}{p^2 + m_l^2}\right]$$

# Results and discussions

| Case | | Parameters | Values | Observables | Values (MeV) |
|---|---|---|---|---|---|
| "Ladder" | $\eta_\psi = 0$ | $m_l$ (MeV) | 0 | $M_q$ | 350.4 |
| | | $\bar{\alpha}_s$ | 0.1529 | | |
| | | $m_l$ (MeV) | 2.76 | $M_q$ | 350.2 |
| | | $\bar{\alpha}_s$ | 0.1493 | $m_\pi$ | 134.9 |
| | | | | $f_\pi$ | 83.2 |
| | $\eta_\psi \neq 0$ | $m_l$ (MeV) | 0 | $M_q$ | 351.1 |
| | | $\bar{\alpha}_s$ | 0.1331 | | |
| | | $m_l$ (MeV) | 2.49 | $M_q$ | 350.1 |
| | | $\bar{\alpha}_s$ | 0.1294 | $m_\pi$ | 135.3 |
| | | | | $f_\pi$ | 80.0 |
| "Non-ladder" | $\eta_\psi = 0$ | $m_l$ (MeV) | 2.57 | $M_q$ | 350.3 |
| | | $\bar{\alpha}_s$ | 0.1640 | $m_\pi$ | 135.0 |
| | | | | $f_\pi$ | 80.6 |
| | $\eta_\psi \neq 0$ | $m_l$ (MeV) | 2.35 | $M_q$ | 350.3 |
| | | $\bar{\alpha}_s$ | 0.1410 | $m_\pi$ | 136.2 |
| | | | | $f_\pi$ | 78.1 |

TABLE I. Parameter fixing in the current work. We demonstrate in the case with "ladder" and "non-ladder", with or without quark anomalous dimension, and also the case of the chiral limit in the "ladder" case.

# Results and discussions

- Phase diagram of dynamical chiral symmetry breaking

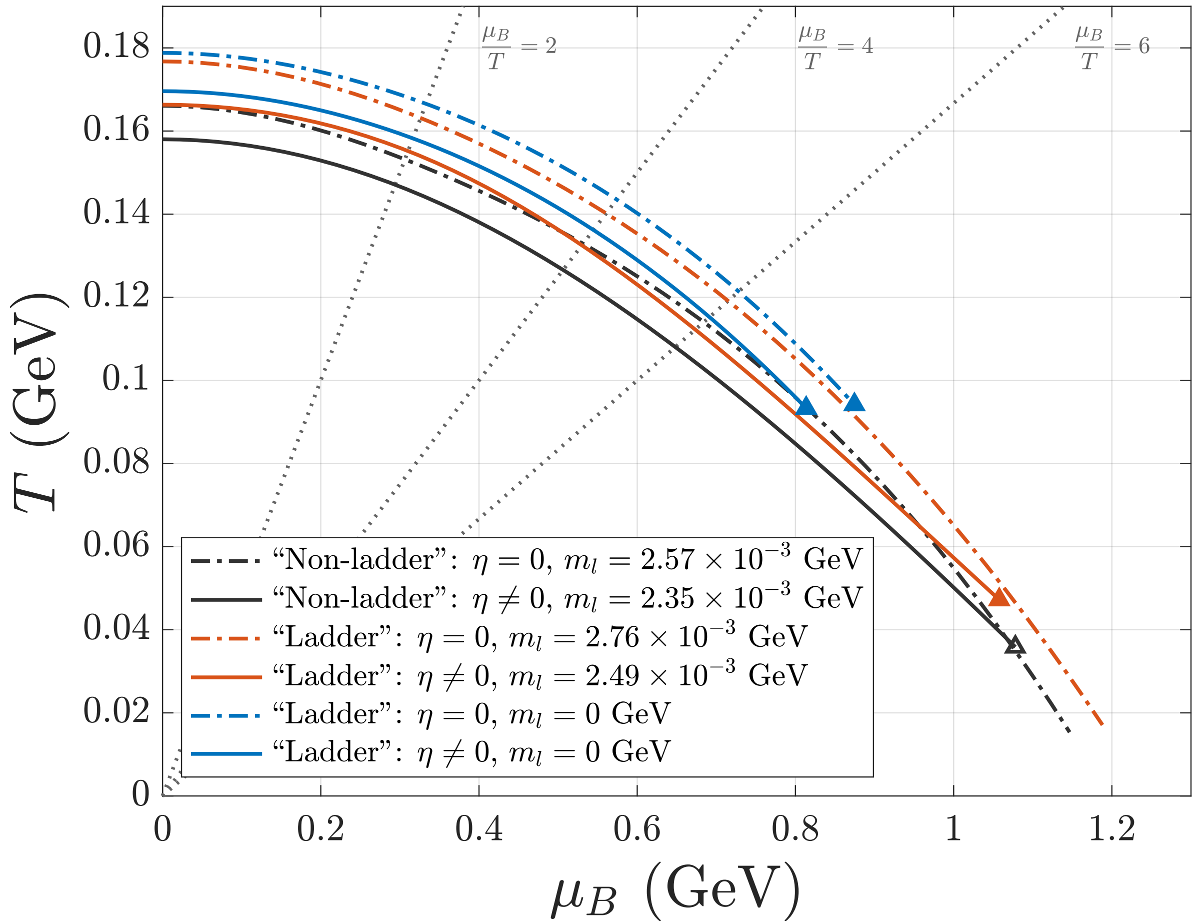

# Results and discussions

## ○ Quantitative results from the phase diagram

- (Psudo-) Phase transition temperature @ vanishing chemical potential

$$T_c(0) = T_c(\mu_B = 0)$$

- Curvature of the transition temperature line ~ vanishing chemical potential

$$\frac{T_c(\mu_B)}{T_c(0)} = 1 - \kappa \left( \frac{\mu_B}{T_c(0)} \right)^2 + \cdots$$

- Position of the critical end point (CEP)

$$(T_c, \mu_{B,c})$$

# Results and discussions

| Cases | | | Observables | Values |
|---|---|---|---|---|
| "Ladder" | $\eta_\psi = 0$ | $m_l = 0$ | $T_c(0)$ (MeV) | 178.8 |
| | | | $\kappa$ | 0.0197 |
| | | | $(T_c, \mu_{B,c})$ (MeV) | (94.16,874.6) |
| | | $m_l \neq 0$ | $T_c(0)$ (MeV) | 176.8 |
| | | | $\kappa$ | 0.0193 |
| | | | $(T_c, \mu_{B,c})$ (MeV) | - |
| | $\eta_\psi \neq 0$ | $m_l = 0$ | $T_c(0)$ (MeV) | 169.6 |
| | | | $\kappa$ | 0.0183 |
| | | | $(T_c, \mu_{B,c})$ (MeV) | (93.31,813.6) |
| | | $m_l \neq 0$ | $T_c(0)$ (MeV) | 166.3 |
| | | | $\kappa$ | 0.0187 |
| | | | $(T_c, \mu_{B,c})$ (MeV) | (47.22,1058) |
| "Non-ladder" | $\eta_\psi = 0$ | $m_l \neq 0$ | $T_c(0)$ (MeV) | 166.1 |
| | | | $\kappa$ | 0.0176 |
| | | | $(T_c, \mu_{B,c})$ (MeV) | - |
| | $\eta_\psi \neq 0$ | | $T_c(0)$ (MeV) | 158.0 |
| | | | $\kappa$ | 0.0198 |
| | | | $(T_c, \mu_{B,c})$ (MeV) | (35.85,1078) |

TABLE II. Observables related to the QCD phase diagram in Figure 7.

# Content

# Summary

- In this work, we revisit the problem of realizing the broken phase in RG method and the QCD phase structure;
- By truncating the IR effective action at the leading order of derivative expansion, we isolate the minimum quarkonic fluctuation we need;
- Utilizing the “ladder” and its beyond, we closed the RG equation at finite temperature and baryon chemical potential;
- Through weak RG formalism, we obtain the weak solution to read off the physical observables;
- We obtain the QCD chiral phase diagram through the dynamical mass:
  - In the vicinity of vanishing baryon chemical potential, the “non-ladder” approx. works well in terms of the phase transition temperature and the curvature of the Tc-line, compared to the other functional approaches;
  - The position of the CEP deviate from those previous approaches, which, in part, is as we expected, indicating the importance of the mesonic fluctuation around the chiral criticality.

Thanks!

# Content

- **Introduction**
- **Functional renormalization group (fRG) setup**
  - FRG setups for QCD fermionic potential: LPA’
  - Gluonic sector and running coupling
- **Searching for the weak solution of fRG equations**
  - Why divergence of 4-fermi matters?
  - Weak form of the RG equations
  - Rankine-Hugoniot condition
  - Method of characteristics
- **Results and discussions**
- **Summary**
- **References**

# References


1. Peter Senger. Probing dense QCD matter in the laboratory—The CBM experiment at FAIR. Phys. Scripta, 95(7):074003, 2020.
2. Wei-jie Fu, Jan M. Pawlowski, and Fabian Rennecke. QCD phase structure at finite temperature and density. Phys. Rev. D, 101(5):054032, 2020.
3. Ken-Ichi Aoki, Keiichi Morikawa, Jun-Ichi Sumi, Haruhiko Terao, and Masashi Tomoyose. Wilson renormalization group equations for the critical dynamics of chiral symmetry. Prog. Theor. Phys., 102:1151–1162, 1999.
4. Jens Braun, Leonard Fister, Jan M. Pawlowski, and Fabian Rennecke. From Quarks and Gluons to Hadrons: Chiral Symmetry Breaking in Dynamical QCD. Phys. Rev. D, 94(3):034016, 2016.
5. Ken-Ichi Aoki, Shin-Ichiro Kumamoto, and Daisuke Sato. Weak solution of the non-perturbative renormalization group equation to describe dynamical chiral symmetry breaking. PTEP, 2014(4):043B05, 2014.
6. C. Wetterich, Exact evolution equation for the effective potential, Phys. Lett. B 301 (1993) 90 [1710.05815].
7. Ken-Ichi Aoki and Daisuke Sato. Solving the QCD non-perturbative flow equation as a partial differential equation and its application to the dynamical chiral symmetry breaking. PTEP, 2013:043B04, 2013.

# References

8. Anton K. Cyrol, Mario Mitter, Jan M. Pawlowski, and Nils Strodthoff. Nonperturbative quark, gluon, and meson correlators of unquenched QCD. Phys. Rev. D, 97(5):054006, 2018.
9. Fei Gao, Joannis Papavassiliou, and Jan M. Pawlowski. Fully coupled functional equations for the quark sector of QCD. Phys. Rev. D, 103(9):094013, 2021.
10. Ken-Ichi Aoki, Shin-Ichiro Kumamoto, and Masatoshi Yamada. Phase structure of NJL model with weak renormalization group. Nucl. Phys. B, 931:105–131, 2018.